1 Supplement of

2 Degradation of anhydro-saccharides and the driving factors

in real atmospheric conditions: A cross-city study in China

4 Biao Zhou ^a, Kun Zhang ^a, Qiongqiong Wang ^b, Jiqi Zhu ^a, Li Li ^{a, *} and Jian Zhen Yu ^{c,d, *} 5 6 7 ^a School of Environmental and Chemical Engineering, Shanghai University, Shanghai, 200444, 8 China 9 ^b Department of Atmospheric Science, School of Environmental Studies, China University of 10 Geosciences, Wuhan, China ^c Department of Chemistry, The Hong Kong University of Science & Technology, Hong Kong, 11 12 China 13 ^d Division of Environment & Sustainability, The Hong Kong University of Science & Technology, 14 Hong Kong, China 15 16 17 18 19 20

- 22 Texts
- 23 Text S1 Standard preparation
- 24 Text S2 Derivation of a decay rate using an inert substance as the reference
- 25 Tables
- 26 Table S1 Online instruments and analysis methods of meteorological parameters, conventional
- pollutants, as well as PM2.5-bound OC/EC and inorganic compounds
- Table S2 A list of corresponding internal standard (IS) and other details for external standards (ESs)
- and compounds in samples
- 30 Table S3 A list of standard preparation details for internal standard (IS) deployed during the
- 31 campaign
- 32 Table S4 Statistics of meteorological conditions, hourly concentrations of conventional atmospheric
- pollutants and TAG measured anhydro-saccharides during the campaign
- Table S5 Daytime decay rates of anhydro-saccharides at three sites calculated using the relative rate
- 35 constant method
- 36 Table S6 GAM smoothing function related parameters
- 37 Figures
- 38 Fig. S1 Locations of the sampling sites
- 39 Fig. S2 Distribution of levoglucosan/K+ ratios and levoglucosan/mannosan ratios from ambient
- 40 measurement, with the corresponding ratios for different kinds of biomass burning types from
- 41 Cheng et al. (2013) (Note that KBB at the Hong Kong site is used as a substitute for K+, with further
- details available in Wang et al., 2025.)
- 43 Fig. S3 Scatter plots showing the correlation between K+BB and decay rates of levoglucosan,
- 44 mannosan, and galactosan in (a) Zibo and (b) Changzhou
- 45 Fig. S4 Correlation of decay rates between levoglucosan, mannosan and galactosan in (a) Zibo, (b)
- 46 Changzhou and (c) Hong Kong
- 47 Fig. S5 Results of residual tests for GAM on the diurnal decay rate of levoglucosan: (a) residual Q-Q
- plot; (b) scatter plot of predicted values vs. residuals; (c) histogram of residuals; (d) scatter plot of
- 49 predicted values vs observed values.

Text S1 Standard preparation

- We use the stock solution for dilution to make the standard, which is all purchased from Anple The working standard solution was freshly prepared by diluting stock solutions several times using 10 mL flasks respectively with ACN and DCM solvent, producing final working solution concentrations are showed in Table S2. Table S2 shows the corresponding IS and other details for external standards (ESs). Table S3 lists the standard preparation details for internal standards.
- Different volumes with range from 5 to 25 µL of working standard solution (ranging from 5 to 25 µL) and a fixed volume (5 µL) of ISs were injected into the collection and thermal desorption cell (CTD) to build calibration curves using the same analysis procedure as that for the samples.

 Calibration curves were constructed by fitting the normalized peak area of ESs to their
- 60 corresponding ISs.

Text S2 Derivation of a decay rate using an inert substance as the reference

The rate expression for the concentration of species *i* in the atmosphere can be written as (Donahue et al., 2005):

$$\frac{\partial c_i}{\partial t} = -k_{ri} \cdot C_{OX} \cdot (1 + f_i) - k_{d_i} \cdot C_i - k_{d'_i} \cdot C_i + E_i$$
 (1)

$$f_i = < \frac{c_{i_{ox}} \cdot c_{i_i}}{c_{ox} \cdot c_i} \tag{2}$$

- k_{ri} is the second-order reaction rate constant of species i in the aerosol, C_i is the measured concentration of species i in the aerosol, C_{OX} is the average oxidant concentration in the aerosol, k_{di} and k_{di} are the dilution and deposition rate constant of the species i, E_i is the source emission rate of species i, f_i is a fractional covariance term that describes spatial variations of the reactants within the particle. f_i is zero if either oxidant or the reactant species i is well mixed (i.e., gradients $C'_{ox} = 0$ or $C'_i = 0$). f_i is greater than zero when species i and oxidant are concentrated at the particle surface. f_i is negative when species i is depleted near the particle surface and the oxidant is concentrated near the particle surface(Huff Hartz et al., 2007).
- The interference from source emissions, atmospheric dilution and deposition can be eliminated by using the concentration ratio of $\frac{c_i}{c_j}$, that is, species i is normalized by a reference species j which showed the same source origins, thus:

77
$$\frac{\partial \frac{C_i}{C_j}}{\partial t} = -\left\{k_{r_i} \cdot C_{OX} \cdot (1+f_i) - k_{r_j} \cdot C_{OX} \cdot (1+f_j)\right\} \cdot \frac{C_i}{C_j} - (k_{d_i} - k_{d_j}) \cdot \frac{C_i}{C_j} - (k_{d'_i} - k_{d'_j}) \cdot \frac{C_i}{C_j} + (E_i - E_j)$$
(3)

Assuming the deposition and dilution rate and fractional covariance term for species i and j are not species dependent, i.e., $k_{d_i} = k_{d_j}$, $k_{d'_i} = k_{d'_j}$, $f_i = f_j$. In our consideration, the species i and j are from the same source. If they show comparable emission rates, i.e., $E_i \cong E_j$, or there are no fresh emissions or emissions are negligible within the consideration timeframe, i.e., $E_i \cong 0$ and $E_j \cong 0$, then:

83
$$\frac{\partial \frac{c_i}{c_j}}{\partial t} = -(k_{ri} - k_{rj}) \cdot (1 + f_i) \cdot C_{OX} \cdot \frac{c_i}{c_j}$$
 (4)

If we consider a scenario where the reaction occurs at or near the aerosol surface, the reagent concentration within the particle is well mixed initially, thus $f_i = 0$ and the following equation holds:

87
$$\frac{\partial \frac{c_i}{c_j}}{\partial t} = -(k_{ri} - k_{rj}) \cdot C_{OX} \cdot \frac{c_i}{c_j}$$
 (5)

Applying the identity $\frac{\partial \ln(x)}{\partial t} = (\frac{\partial x}{\partial t}) \cdot (\frac{1}{x})$, and Equation 5 can be rewritten as:

89
$$\frac{\partial \ln(C_i/C_j)}{\partial t} = -(k_{ri} - k_{rj}) \cdot C_{OX}$$
 (6)

To determine the decay rate of the BB-emitted saccharides, we select the K^{+}_{BB} as the reference species j. K^{+}_{BB} is inert to the oxidants ($k_{rj} = 0$), thus:

92
$$\frac{\partial \ln(c_i/c_{K^+_{BB}})}{\partial t} = -k, k = k_{ri} \cdot C_{OX}$$
 (7)

Table S1 Online instruments and analysis methods of meteorological parameters, conventional pollutants, as well as PM_{2.5}-bound OC/EC and inorganic compounds

Instrument	Machine type	Manufacturer	Monitoring factors	Analytical Principle		
		Zibo, Shandong pr	ovince, NCP			
PM _{2.5} online monitor	MODEL 5014i	Thermo Fisher Scientific, US	PM _{2.5}	Beta-ray method		
NO _x analyzer	MODEL 42i	Thermo Fisher Scientific, US	NO, NO ₂ , NO _x	Pulsed fluorescence method		
Ozone Analyzer	MODEL 49i	Thermo Fisher Scientific, US	O_3	Differential absorption spectroscopy		
Aerosol compositions monitor	MODEL S611	Fortelice International Co., Ltd., Taiwan, China	C1-、 NO_3 -、 SO_4 2-、 Na +、 NH_4 +、 K +、 Mg^{2+} 、 Ca^{2+}	Ion chromatography		
OC/EC online monitor	MODEL ECOC - 610	Hangzhou Pengpu Technology Co., Ltd., China	OC、EC	Thermal light Method		
Meteorological monitor	\	China Meteorological Administration	WS、WD、RH、T、P、 RF	https://www.cma.gov.cn/		
Solar radiation analyzer	CMP11	Kipp & Zonen, Zuid - Holland, Netherlands	SSRD	Pulsed light signal method		
Changzhou, Jiangsu province, YRD						
Meteorological monitor	WXT520	VAISALA, FL	WS、WD、RH、T、P、 RF	Ultrasonic and capacitive measurement methods		
PM _{2.5} online monitor	BAM1020	Met One, US	PM _{2.5}	Beta-ray method		
Ozone Analyzer	MODEL 49i	Thermo Fisher Scientific, US	O_3	Differential absorption spectroscopy		
NO _x analyzer	MODEL450i	Thermo Fisher Scientific, US	NO, NO ₂ , NO _x	Pulsed fluorescence method		
OC/EC online monitor	RT-4	Sunset Laboratory, US	OC, EC	Thermal light Method		
MARGA ionic online analyzer	ADI2080	Metrohm, CHN	$\begin{array}{cccccccccccccccccccccccccccccccccccc$	Ion chromatography		
		HongKong,	PRD			
MARGA ionic online analyzer	ADI2080	Metrohm, CHN	Cl $^{-}$, NO $_{3}^{-}$, SO $_{4}^{2-}$, Na $_{}^{+}$, NH $_{4}^{+}$, K $_{}^{+}$, Mg $_{}^{2+}$, Ca $_{}^{2+}$	Ion chromatography		
OC/EC online monitor	RT-4	Sunset Laboratory, US	OC、EC	Thermal light Method		
PM _{2.5} online monitor	Model 5030i	Thermo Fisher Scientific, US	PM _{2.5}	Beta-ray method		
Gas pollutants analyzer	AWS tower	Hong Kong Environment	WS, WD, RH, T, P, RF, O_3 , SSRD, SO_2 ,	\		

Protection Department	NO.	NO_{2}	NO.
I Totection Department	TNO.	11021	1100x

elemental		Cooper Environmental		
species	Xact 625i	Services	K, Ca	X-ray method
analyzer		Scrvices		

Table S2 A list of corresponding internal standard (IS) and other details for external standards (ESs) and compounds in samples

Compound	Formula	Solvent	Quantification IS	Working solution (ng/μL).	Quantification ion
Levoglucosan	C6H10O5	DCM+		0.294	204
Galactosan	C6H10O5	ACN	Levoglucosan-d7	0.293	217
Mannosan	C6H10O5			0.294	204

Table S3 A list of standard preparation details for internal standard (IS) deployed during the campaign

Compound	Formula	Solvent	Working solution	Quantification	
Compound	rormuia	Solvent	$(ng/\mu L)$	ion	
Levoglucosan-d7	C6H3D7O5	DCM + ACN	1.046	206	

Table S4 Statistics of meteorological conditions, hourly concentrations of conventional atmospheric pollutants and TAG measured anhydro-saccharides during the campaign

Measurement parameters	ZB	CZ	НК
$PM_{2.5} (\mu g/m^3)$	69.4±58.0	49.9±26.4	20.5±8.8
T (°C)	-0.2±6.1	10.9±4.9	19.6±5.2
RH (%)	52.1±22.3	56.6±18.4	68.4±17.51
$NO_2\left(\mu g/m^3\right)$	44.4±24.6	45.2±24.8	5.8 ± 6.6
$O_3 (\mu g/m^3)$	59.2±16.2	68.9±26.7	56.9±12.2
WS (m/s)	2.2±1.7	1.3±0.7	3.3±1.7
$SO_4^{2\text{-}}\big(\mu g/m^3\big)$	8.8±7.3	6.3±2.7	9.4±8.3
$NO_3^-(\mu g/m^3)$	15.0±15.2	17.6±11.7	2.5±2.6
OC ($\mu g/m^3$)	7.7±4.9	6.0±3.7	3.6±2.0
EC (µg/m³)	3.3±2.4	1.9±1.4	1.2±0.8
Levoglucosan (ng/m³)	45.5 ± 32.3	45.1±38.7	27.6±15.6
Mannosan (ng/m³)	2.4±1.7	3.6±3.2	1.9±1.5
Galactosan (ng/m³)	4.5±3.4	2.4±2.0	0.9 ± 0.7

Table S5 Daytime decay rates of anhydro-saccharides at three sites calculated using the relative rate constant method

Decay of anhydro-saccharides	ZB	CZ	НК
k_lev	0.103 ± 0.027	0.126 ± 0.052	0.097 ± 0.011
k_man	0.095 ± 0.033	0.128 ± 0.070	0.137 ± 0.015
k_gal	0.105 ± 0.034	0.133 ± 0.082	0.147 ± 0.016

113 Table S6 GAM smoothing function related parameters

Smooth variables	Edf	Ref.df	F	p		
ALWC	1.0	9.0	5.2	0.02		
T	2.5	9.0	8.7	0.001		
O_x	1.8	9.0	6.5	0.01		
RH	3.2	9.0	3.1	0.08		
SSRD	4.0	9.0	2.3	0.12		
Deviance explained (%) =70.9%						
$R^2=0.70$						

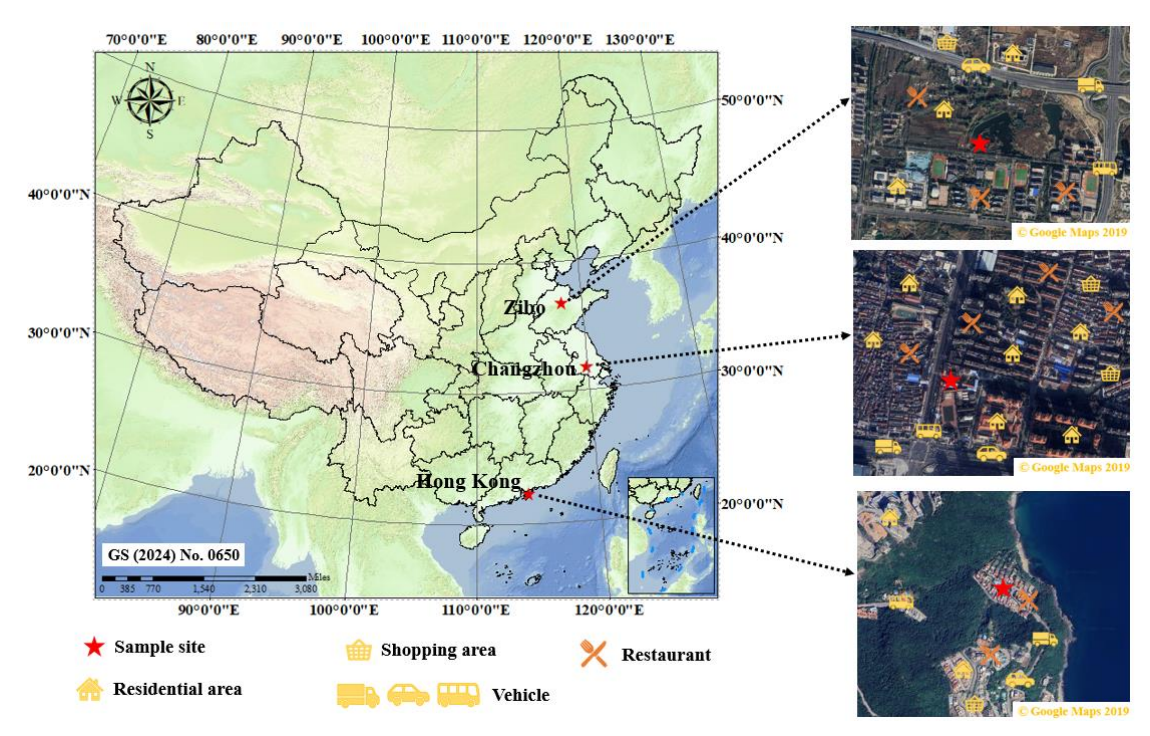


Fig. S1 Locations of the sampling sites. Base map from China National Public Service Platform for Geoinformation, satellite imagery © Google Maps, 2019.

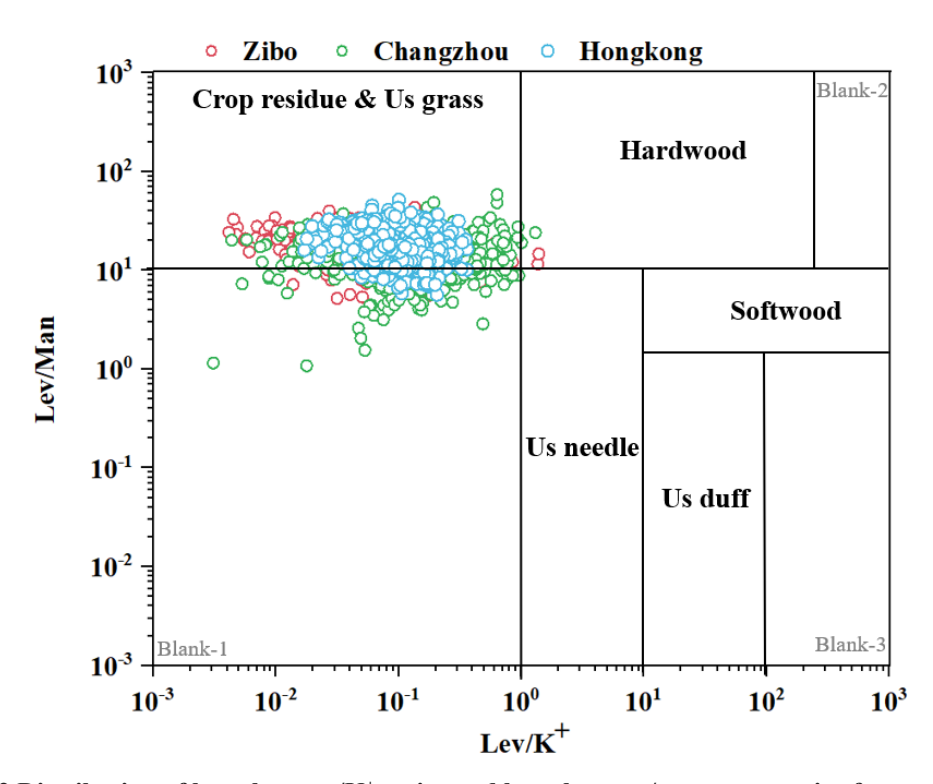


Fig. S2 Distribution of levoglucosan/ K^+ ratios and levoglucosan/mannosan ratios from ambient measurement, with the corresponding ratios for different kinds of biomass burning types from Cheng et al. (2013) (Note that K_{BB} at the Hong Kong site is used as a substitute for K^+ , with further details available in Wang et al., 2025.)

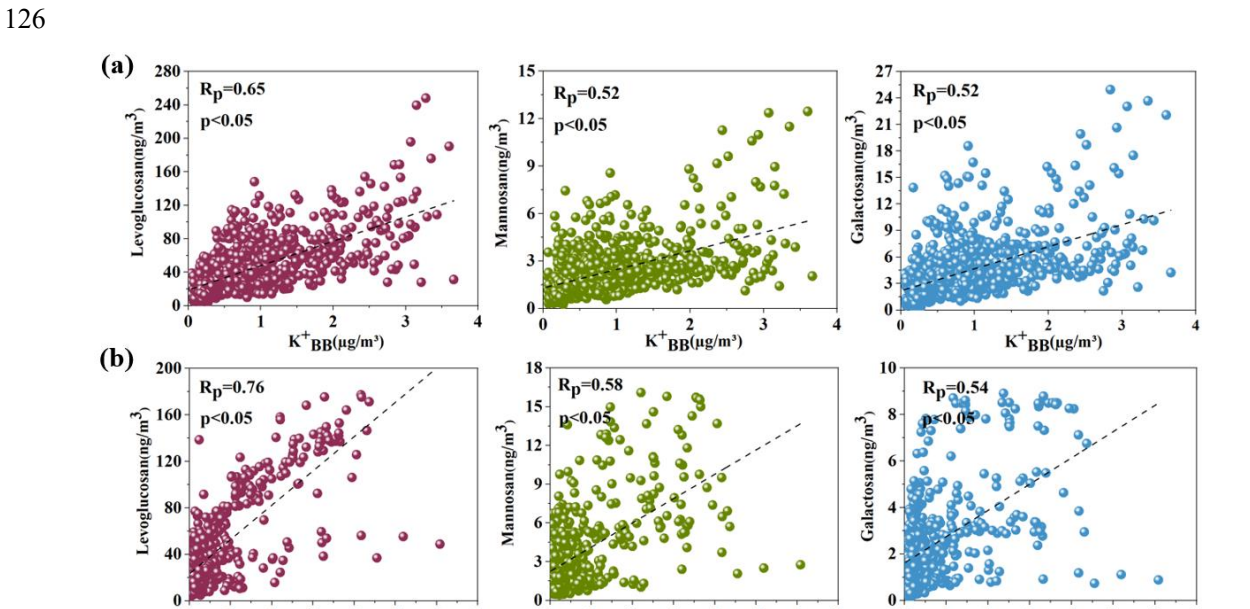


Fig. S3 Scatter plots showing the correlation between K^+_{BB} and decay rates of levoglucosan, mannosan, and galactosan in (a) Zibo and (b) Changzhou

 $K^{+}BB(\mu g/m^{3})$

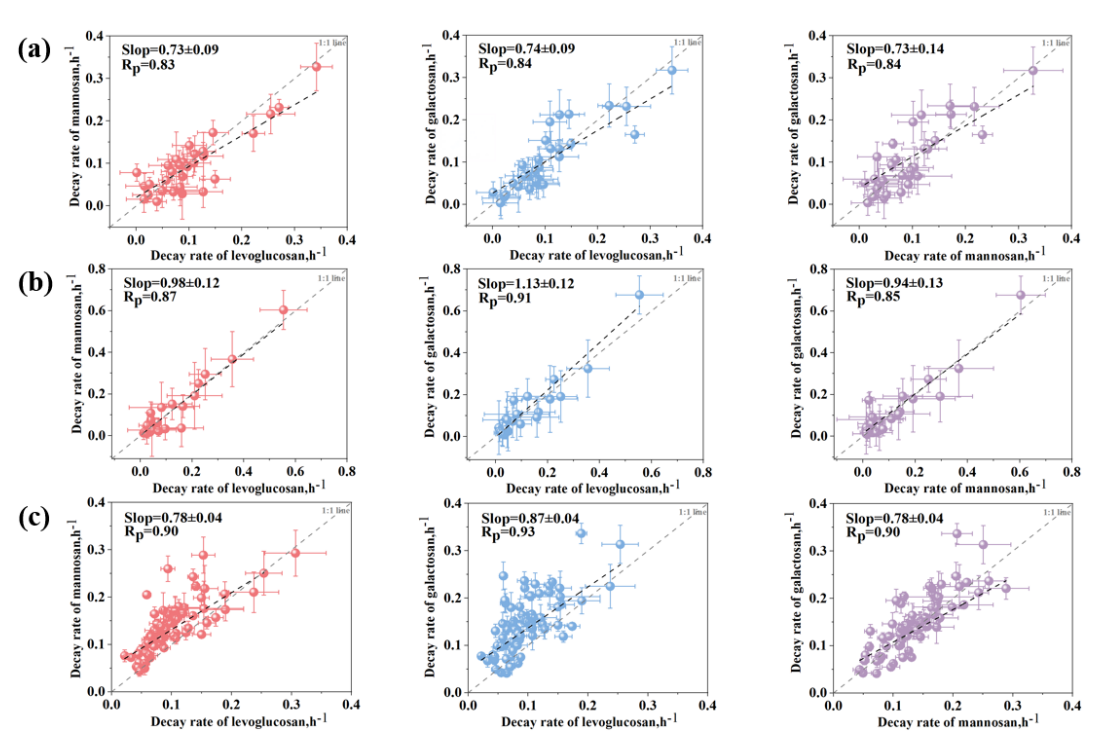


Fig. S4 Correlation of decay rates between levoglucosan, mannosan and galactosan in (a) Zibo, (b) Changzhou and (c) Hong Kong

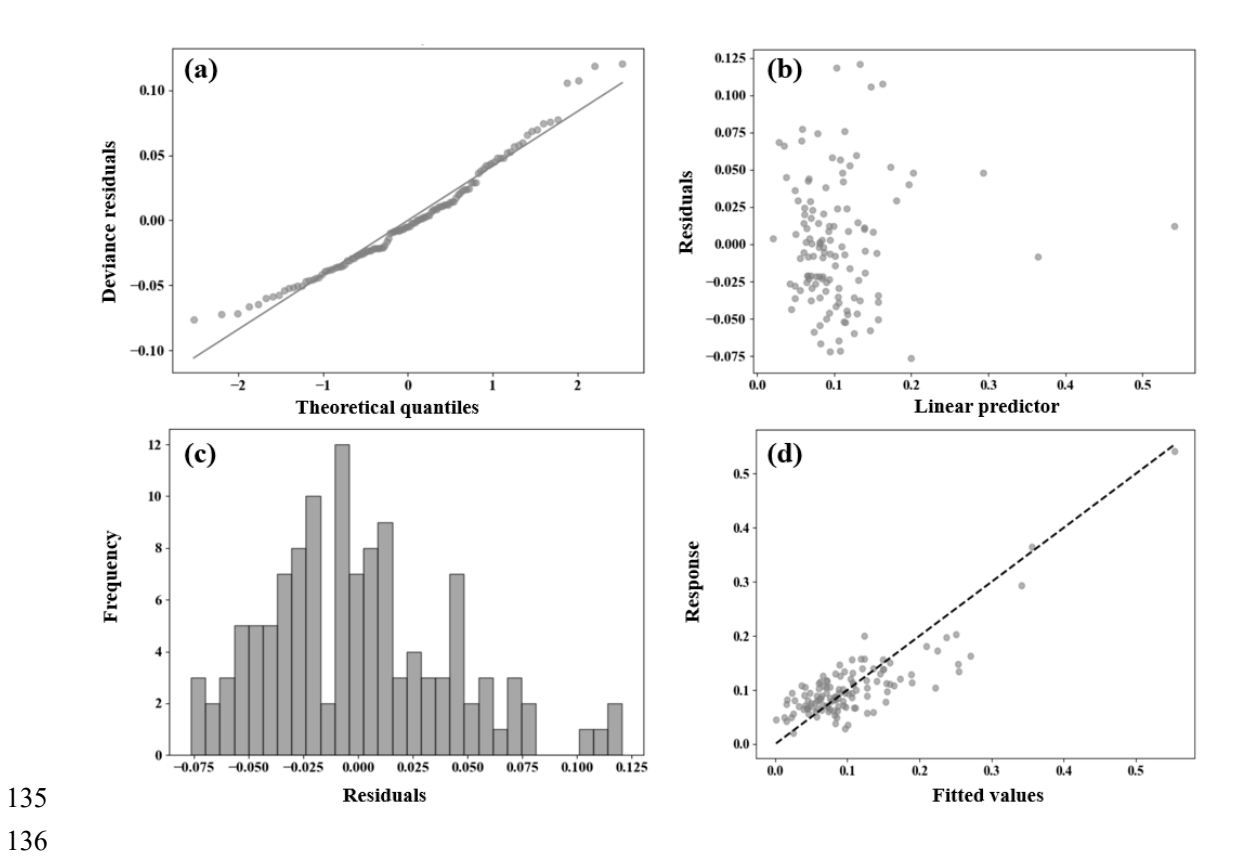


Fig. S5 Results of residual tests for GAM on the diurnal decay rate of levoglucosan: (a) residual Q-Q plot; (b) scatter plot of predicted values vs. residuals; (c) histogram of residuals; (d) scatter plot of predicted values vs observed values

References

- Donahue, N.M., Robinson, A.L., Hartz, K.E.H., Sage, A.M., Weitkamp, E.A., 2005. Competitive
- oxidation in atmospheric aerosols: The case for relative kinetics, Geophys. Res. Lett., 32.
- 145 http://dx.doi.org/10.1029/2005gl022893.
- Huff Hartz, K.E., Weitkamp, E.A., Sage, A.M., Donahue, N.M., Robinson, A.L., 2007. Laboratory
- measurements of the oxidation kinetics of organic aerosol mixtures using a relative rate constants
- 148 approach, J. Geophys. Res.:Atmos., 112. http://dx.doi.org/10.1029/2006jd007526.
- Li, Q., Zhang, K., Li, R., Yang, L., Yi, Y., Liu, Z., Zhang, X., Feng, J., Wang, Q., Wang, W., Huang, L.,
- Wang, Y., Wang, S., Chen, H., Chan, A., Latif, M.T., Ooi, M.C.G., Manomaiphiboon, K., Yu, J., Li, L.,
- 151 2023. Underestimation of biomass burning contribution to PM2.5 due to its chemical degradation based
- on hourly measurements of organic tracers: A case study in the Yangtze River Delta (YRD) region, China.
- Science of The Total Environment. 872. http://dx.doi.org/10.1016/j.scitotenv.2023.162071.
- Wang, Q., Wang, S., Chen, H., Zhang, Z., Yu, H., Chan, M.N., Yu, J.Z., 2025. Ambient Measurements of
- Daytime Decay Rates of Levoglucosan, Mannosan, and Galactosan, J. Geophys. Res.:Atmos., 130.
- 156 http://dx.doi.org/10.1029/2024jd042423.
- Wang, Q., &Yu, J.Z., 2021. Ambient Measurements of Heterogeneous Ozone Oxidation Rates of Oleic,
- Elaidic, and Linoleic Acid Using a Relative Rate Constant Approach in an Urban Environment, Geophys.
- Res. Lett., 48. http://dx.doi.org/10.1029/2021gl095130.
- Williams, B.J., Goldstein, A.H., Kreisberg, N.M., Hering, S.V., 2006. An In-Situ Instrument for Speciated
- Organic Composition of Atmospheric Aerosols: Thermal Desorption Aerosol GC/MS-FID (TAG).
- Aerosol Science and Technology. 40, 627-638. http://dx.doi.org/10.1080/02786820600754631.